Temperature dependence of the nuclear quadrupole interactions at Ti sites in ferroelectric $PbTiO_3$ and in ilmenite and perovskite $CdTiO_3$: Evidence for order-disorder phenomena

Gary L. Catchen, Stephen J. Wukitch, and David M. Spaar
Department of Nuclear Engineering, and Center for Electronic Materials and Processing, The Pennsylvania State University, University Park, Pennsylvania 16802

Michael Blaszkiewicz
Materials Research Laboratory, The Pennsylvania State University, University Park, Pennsylvania 16802
(Received 10 November 1989; revised manuscript received 8 February 1990)

Perturbed angular correlation (PAC) spectroscopy was used to measure electric-field gradients (EFG's) at Ti sites in the tetragonally distorted perovskite $PbTiO_3$, which is ferroelectric, and in the orthorhombically distorted perovskite $CdTiO_3$, and the ilmenite $CdTiO_3$, which are not ferroelectric. The PAC probe $^{181}Hf/^{181}Ta$ was substituted into Ti sites in these phases at concentrations of approximately 1% of the Ti concentrations. Nuclear quadrupole interactions were measured from 77 to 730 K for the $PbTiO_3$ phase and from 77 to ~ 1260 K for the $CdTiO_3$ phases. The perturbation functions for $PbTiO_3$ are characterized by high frequencies that show near-axial symmetry and that decrease rapidly at temperatures near the ferroelectric-to-paraelectric transition temperature T_c. Also, they are characterized by extensive line broadening that increases at temperatures near T_c. The perturbation functions for the perovskite $CdTiO_3$ are characterized by low frequencies that show much asymmetry $\eta \cong 0.4$ and by little line broadening, and the associated EFG decreases linearly with temperature. For the ilmenite $CdTiO_3$, the perturbation functions are characterized by moderate frequencies that show near-axial symmetry and by very little line broadening, and the associated EFG decreases with the three-halves power of the temperature. For both of the $CdTiO_3$ phases, the asymmetries derived from the measured frequencies are consistent with the crystal-structure symmetries, and the line shapes could be attributed to static inhomogeneities. For the ferroelectric $PbTiO_3$ phase, the measured frequencies are consistent with the tetragonal crystal structure. But, the line shapes of the perturbation functions measured at temperatures near T_c could not be explained by purely static inhomogeneities. Instead, in contrast to the $CdTiO_3$ phases, the line broadening at these temperatures was attributed primarily to a dynamic spin-relaxation mechanism. This particular interpretation supports an order-disorder model of the ferroelectric phenomenon.

I. INTRODUCTION

Since the 1950's, the soft-mode model has been the generally accepted description of phase transitions in ABO_3 perovskite crystals such as barium titanate and lead titanate.[1,2] In this model, the paraelectric-to-ferroelectric phase transition arises from a lattice-vibrational instability. The unstable mode goes to zero frequency at the Curie temperature T_c, and the lattice distorts into a lower-symmetry structure in which the symmetry reflects the symmetry of the unstable soft mode. In most cases, in the crystallographic analysis, the paraelectric phase represents a cubic, i.e. "true," perovskite; and the ferroelectric phase represents a distorted, lower-symmetry perovskite. Thus, according to the soft-mode model, the transition from the paraelectric phase to the ferroelectric phase is a *static,* displacive process.

In contradistinction, the order-disorder model describes the phase transition as a *dynamic* process, which other investigators have suggested.[3] Recently, Sokoloff, Chase, and Rytz[4] used an eight-site, dynamic order-disorder model to interpret inelastic light scattering measurements on $KNbO_3$ and $BaTiO_3$, which is based on a static disorder model that Comes, Lambert, and Guinier initially proposed over two decades ago.[5,6] In this model, the B ion moves between locations that correspond to minima in a potential-energy surface. These minima are displaced symmetrically from the crystallographic B site. The B-ion occupation probabilities associated with these minima determine the phase. Equal occupation probability corresponds to the disordered phase, which is referred to as being "cubic," and unequal occupation probability corresponds to the ordered, lower-symmetry phase.

The experimental situation is far from clear. Earlier, in a recent communication, we described several experiments (besides the aforementioned inelastic light scattering experiment[4]) that show evidence for the Ti ions being off center in the cubic phase of $BaTiO_3$.[7] This evidence suggests that the cubic crystallographic structure represents a macroscopic, average picture of the crystal. Also, Burns and Scott,[3] who used Raman spectroscopy to investigate lattice modes in $PbTiO_3$, pointed out that the transition in $PbTiO_3$ ". . . appears to be a textbook exam-

ple of a displacive ferroelectric phase transition." In the tetragonal, ferroelectric phase of $PbTiO_3$, the lattice modes are sharp and underdamped, and they obey the Raman selection rules. However, the soft mode in tetragonal $BaTiO_3$ is overdamped (in the context of the damped-harmonic-oscillator model).[3] This difference cannot be explained by a purely displacive phase-transition mechanism. Moreover, as a result of their analysis, Burns and Scott also mentioned that Raman measurements have not provided evidence for critical effects in first-order phase transitions in $PbTiO_3$ and $BaTiO_3$.[3] To reconcile this information, the effects of local fields at the B sites in the ABO_3 ferroelectrics need to be investigated in the context of phase-transition mechanisms.

We have used PAC spectroscopy to continue the initial study[7] of ABO_3 perovskites. The general objective has been to investigate paraelectric-to-ferroelectric phase transitions, and the specific objective has been to discern dynamic order-disorder phenomena from static displacive effects that are associated with these phase transitions. In particular, the PAC technique can measure static and time-varying nuclear electric quadrupole interactions. These interactions take place between the nuclear quadrupole moments of radioactive probe atoms, that were substituted into specific lattice sites in the structure, and the extranuclear electric-field gradients (EFG's). Analysis of the EFG's produced by static interactions can provide information about the strength and symmetry of the local crystal field. In contrast to static interactions, time-varying interactions, which arise when the EFG's fluctuate in either magnitude or symmetry during the nuclear probe lifetime, cause the nuclear spin orientations to relax. This effect, which can be caused by effects such as ions "hopping" in and out of lattice sites, attenuates the measured angular correlation. In the analysis, often a correspondence can be made between the measured attenuation rate and the frequency of the motion that produced the attenuation. In this context, then, we associate the effects of displacive phase transitions with static electric quadrupole interactions and the effects of order-disorder phenomena with time-varying interactions and the associated spin relaxation.

Although conceptually the distinction between static interactions associated with displacive transitions and spin-relaxation effects associated with order-disorder phenomena is clear, these different effects may be experimentally ambiguous. Sharp lines, from which a well-defined quadrupole frequency and asymmetry parameter can be derived, characterize static interactions. Whereas, relaxation effects can give rise to broadened, attenuated lines. Alternatively, broadened lines may arise from static inhomogeneities, i.e., from impurities and defects. Since all real solids contain some impurities and defects, observing line broadening in PAC measurements on solids is neither unusual nor unexpected. To interpret the linebroadening as arising from nuclear spin relaxation requires information that can be used to rule out static effects.

Moreover, as our initial study showed, which also reviewed the previously reported PAC experiments,[7] the ABO_3 perovskites tend to show a significant amount of line broadening in the ferroelectric phases. For example, in the early studies, the line broadening measured on tetragonal $PbTiO_3$ was attributed to static inhomogeneities. But, later measurements of the temperature sensitivity of the line broadening suggested that in the particular case of $PbTiO_3$ the line broadening resulted from a thermally activated spin-relaxation mechanism.[7] Also, in these materials, the EFG temperature dependence tends to show critical behavior near T_c.[8] In addition, the high-temperature paraelectric phases of these perovskites tend to show very weak perturbations that are not temperature sensitive.[7] Interpreting this particular feature is problematical at this point, since the experimental results do not lend singular support to either a static or a dynamic mechanism.

To clarify at least part of this situation, this information prompted us to consider two not unrelated questions: (1) can the line broadening observed in the tetragonal, ferroelectric phase of $PbTiO_3$ be attributed primarily to dynamic effects?, and (2) are line-broadening phenomena primarily a result of dynamic order-disorder effects in ferroelectric phases which are absent in similar nonferroelectric phases? Because critical behavior of the EFG temperature dependence near T_c was observed, for example, in PbHfO,[8] an additional question arises: Can the EFG temperature dependence be represented by any conventional theory?[9]

In this context, studying $PbTiO_3$ has a particular advantage. The temperature range of the tetragonal, ferroelectric phase of $PbTiO_3$ is the largest known; it ranges from below 77 to 766 K.[1] This property allows the temperature dependence of line-broadening phenomena and the corresponding temperature dependence of the EFG to be studied over a large temperature range in a single phase. In $PbTiO_3$, the soft mode is underdamped,[1,3] and lattice vibrations follow the Raman selection rules closely.[3] This conventional behavior is not the case for $BaTiO_3$, for example.[1,3] Thus, this feature of $PbTiO_3$ provides a means determining whether a relationship exists between the temperature dependence of the EFG and the nature of the lattice modes, which are well defined in the $PbTiO_3$ structure.

To investigate the relationship between crystal structure, ferroelectricity, and line broadening, $CdTiO_3$ has a singular advantage. Over the temperature range of interest, >77 K, $CdTiO_3$ is not ferroelectric [although a ferroelectric phase transition may occur at about 50 K (Ref. 10)]. More importantly, unlike incipient ferroelectrics such as $SrTiO_3$, $CdTiO_3$ does not crystallize into a cubic structure. Instead, $CdTiO_3$ crystallizes into an orthorhombically distorted perovskite structure, when it is sintered above approximately 1320 K; and $CdTiO_3$ crystallizes into an ilmenite structure, when it is sintered below approximately 1270 K.[11] Figure 1 presents diagrams of these structures. These two structures differ appreciably in symmetry and in oxygen coordination. The perovskite structure is very asymmetric, $a=5.348$ Å, $b=7.615$ Å, $c=5.417$ Å;[12] and the Ti ion and the Cd ion are six and twelve coordinate, respectively. Whereas, the ilmenite structure has a threefold axis of rotational sym-

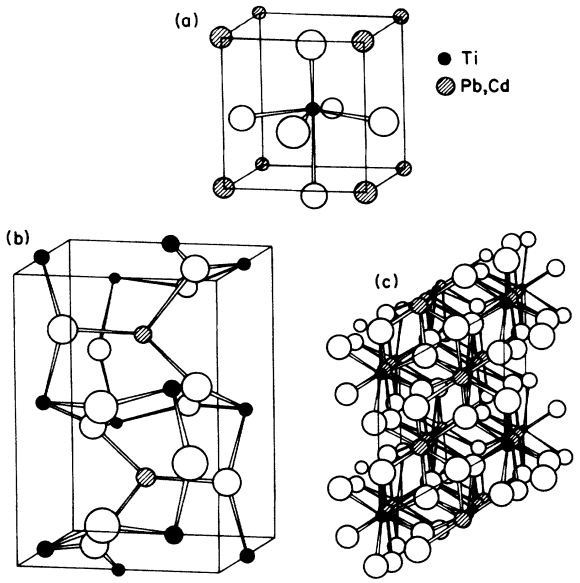

FIG. 1. (a) Diagram of the $PbTiO_3$ tetragonally distorted perovskite structure. (b) Diagram of the $CdTiO_3$ orthorhombically distorted perovskite structure. (c) Diagram of the $CdTiO_3$ ilmenite structure viewed (nearly) along the threefold axis of rotational symmetry.

metry, $a = 5.2403$ Å and $c = 14.838$ Å;[13] and the Ti ion and the Cd ion are both six coordinate. Since both the perovskite and the ilmenite structures can be prepared from the same powder, any differences in line broadening observed in the two structures cannot be attributed to differences in the impurity contents. The differences, therefore, must result from either the effects of defects or inherent structural differences, or perhaps both. Also, we expect Hf to substitute for Ti in small amounts, 1–2 %, in $PbTiO_3$ and in $CdTiO_3$. In what follows, we present PAC measurements that were made using the $^{181}Hf/^{181}Ta$ PAC probe. The specific materials that we investigated were ferroelectric $PbTiO_3$ in the tetragonal perovskite phase and nonferroelectric $CdTiO_3$ in the orthorhombic perovskite phase and in the ilmenite phase. We compare the effects of temperature on the electric quadrupole interactions at Ti sites in these three materials.

II. EXPERIMENTAL DETAILS

A. Sample preparation

Samples of $PbTiO_3$ and $CdTiO_3$ were prepared using a variation of the resin-intermediate method.[14] A major advantage of this method over the conventional method that involves the solid-state reaction of oxide powders is that the probe ions along with the metal ions are mixed homogeneously in solution. Presumably, the homogeneity is retained during the resin formation and the subsequent pyrolysis and calcination.

Typically, batches of 10–15 g of product were prepared using the following procedure. An aqueous solution of either $Cd(NO_3)_2$ or $Pb(NO_3)_2$ was added to a commercially prepared solution of citric acid, ethylene glycol, and titanium alkoxide. To this solution, approximately 1 mCi of the radioactive ^{181}Hf probe was added as several hundred milligrams of $HfOCl_2$ dissolved in H_2O. The nominal Hf concentrations were 0.5–1 % of the *B*-ion concentrations. The solution was heated on an electric hot plate until a thick resin was formed. Then, the resin was pyrolyzed, and the residue was calcined in a box furnace at approximately 1070 K for 8–24 h. Because the c/a ratio of the $PbTiO_3$ structure is large, $\cong 1.06$, sintered pellets are not easily produced from pure $PbTiO_3$ powders. For this reason, powder samples of $PbTiO_3$ were prepared and measured. In the case of $CdTiO_3$, sintered pellets were prepared. The calcined powder was pressed into pellets approximately 6 mm in diameter and several mm thick. The pellets were sintered in an alumina boat that was inserted into a tube furnace. To reduce the volatility of Cd, prior to sintering, some CdO powder was added to the boat and the tube ends were closed. As we discuss in the following, this practice was probably not completely effective. From experience, we found that sintering at a temperature of approximately 1230 K yielded a phase-pure ilmenite structure. Sintering at temperatures above 1400 K, produced the perovskite structure. Sintering at temperatures in between this range, generally produced mixed-phase products. Similarly, in this temperature range, $CdTiO_3$ undergoes a reconstructive phase transition that has not been well characterized. To check the phase purity of the $PbTiO_3$ powder and the $CdTiO_3$ sintered pellets, generally, x-ray powder diffraction patterns were measured on small amounts of radioactive powder that were taken from the respective PAC samples. To perform the PAC measurements, sample material that typically contained 15–30 μCi of ^{181}Hf activity was sealed in fused-silica tubes. To perform the elevated-temperature PAC measurements, a simple tube furnace was used to maintain the temperature. Although a commercial device was used to control the temperature via a type-*S* thermocouple, temperature drifts of 5–10 K during the measurement period of 1–2 d were observed.

B. PAC measurements

Most of the experimental details can be found in a recent paper.[15] Here, we present the relevant details. In particular, the four-CsF-detector apparatus was used to collect eight (four 90° and four 180°) coincidences concurrently. The experimental perturbation functions $A_{22}G_{22}(t_i)$ were obtained from the measured correlation functions $W_{jk}(\theta_{jk}, t_i)$ that represented the primary experimental data (the subscripts j and k refer to the coincidence between the respective detectors and i refers to the time interval). Specifically, the ratio method was used to obtain $A_{22}G_{22}(t_i)$, which Eqs. (1) and (2) in Ref. 15 describe.

To obtain the quadrupole frequencies ω_Q and the asymmetry parameters from the experimental perturbation functions, generally, a two-site model was used to fit the data:

$$A_{22}G_{22}(t_i)=A_1[S_0+\sum_{k=1}^{3}S_k\exp(-\tfrac{1}{2}\omega_k\delta_1 t_i)\cos(\omega_k t_i)]+A_2[S_0+\sum_{k=4}^{6}S_k\exp(-\tfrac{1}{2}\omega_k\delta_2 t_i)\cos(\omega_k t_i)]+A_3\ . \quad (1)$$

A_1 and A_2 are the normalization factors. A_3 takes into account the fraction of probe atoms that are not in well-defined chemical environments, i.e., A_3 represents the "hard core" to which the corresponding perturbation function decays. δ_1 and δ_2 are the line-shape parameters. The frequencies ω_k and the S_k coefficients describe a static interaction in a polycrystalline source. The interaction frequencies ω_k, which are obtained by fitting Eq. (1) to the experimental perturbation functions, are used to calculate the quadrupole frequency ω_Q and the asymmetry parameter η. The calculation of the S_k coefficients is described elsewhere.[16,17] The quadrupole frequency ω_Q is related to the zz component of the EFG, V_{zz}, in the principal-axis system (where the probe nucleus is at the origin) by

$$\omega_Q=[eQV_{zz}/4I(2I-1)\hbar]\ ,$$

in which Q is the nuclear quadrupole moment (2.51b) and I is the nuclear spin. The asymmetry parameter $\eta=(V_{xx}-V_{yy})/V_{zz}$ describes the deviation of the EFG from axial symmetry; also $0\le\eta\le 1$, in which $\eta=0$ characterizes an EFG that has an axis of threefold or higher rotational symmetry. In addition, some of the perturbation functions also were fit using Gaussian line-shape factors, $\exp(-\frac{1}{2}(\delta\omega_k t_i)^2)$, in place of the Lorentzian factors, $\exp(-\frac{1}{2}\omega_k\delta t_i)$, in Eq. (1).

III. RESULTS

Figure 2 presents several perturbation functions for a $PbTiO_3$ powder sample that were measured over a range of temperatures below the Curie temperature (766 K).[11] These data were fit using a one-site model, i.e., Eq. (1) with $A_2=0$. Because the structure of $PbTiO_3$ is tetragonal in this temperature range and has one type of Ti site, the one-site model is appropriate. Moreover, the quality of the fits is very good. The derived values of A_1 and A_3 indicate that (90±5)% of the probes occupied a specific lattice site, and chemical considerations indicate that the site was the Ti site. For these perturbation functions, Fig. 3 summarizes the EFG parameters V_{zz} and η, that the frequency parameters derived from the fits represent, and the line-shape parameter δ. The asymmetry parameters are small, <0.15. When the EFG is characterized by a single set of interaction frequencies ω_k and by axial symmetry, the asymmetry parameter should vanish. However, when a distribution of frequency sets occurs that represents average axial symmetry, the experimental consequence is that a small but nonvanishing asymmetry is observed. Thus, the result is consistent with the axial symmetry that characterizes the Ti site in the tetragonal structure of $PbTiO_3$. The EFG decreases with temperature. Above 600 K, the decrease appears to be much more rapid than below 600 K. This feature of the data suggests that as $PbTiO_3$ approaches the Curie temperature, critical phenomena begin to occur. However, because the temperature control used in these measurements was crude, we were not able to make reliable measurements at temperatures near T_c. Thus, in the context of $PbTiO_3$, we were not able to explore critical phenomena adequately. Aside from the difficulties associated with measurements at temperatures near T_c, the line-broadening effects over the entire temperature range appear to be extensive. The line-shape parameters are approximately 0.1 at temperatures below 600 K, and above

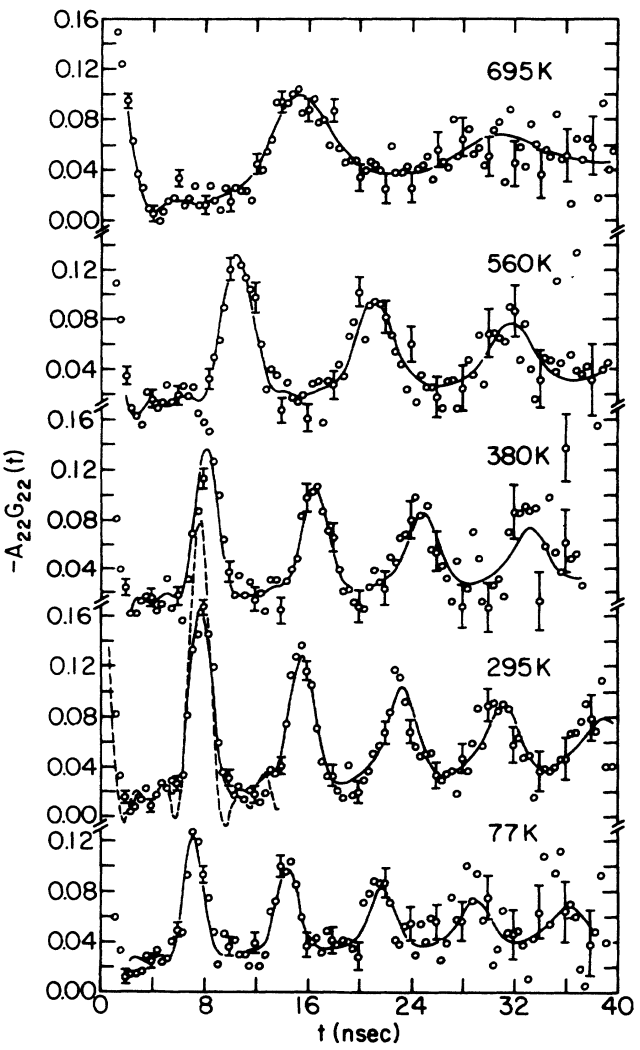

FIG. 2. Perturbation functions for a $PbTiO_3$ powder sample, which were measured at the indicated temperatures. The solid lines represent least-squared fits of Eq. (1) (which includes Lorentzian line-broadening factors) to the data. The data measured at 77 K show less anisotropy than these measured, for example, at 295 K. Most likely, this effect resulted from γ rays that scattered in either the Dewar flask or the liquid nitrogen en route to the detector. On the data measured at 295 K, the dotted line (shown for one period) indicates a fit in which $\delta=0$ and the other parameters are the same as for the solid line fit.

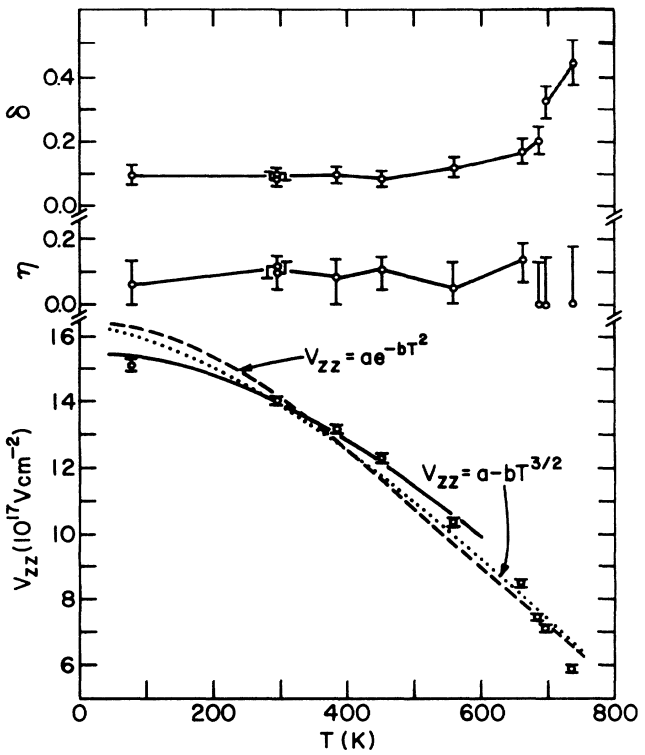

FIG. 3. Electric-field-gradient parameters and line-shape parameters, that correspond to the perturbation functions shown in Fig. 1. For the η and δ data, the lines are drawn to guide the eye. For the V_{zz} data, the lines represent fits to the indicated functions. The solid line represents a fit of either function to the data points for which $T < 600$ K.

600 K they increase. To emphasize this point, a second line was calculated for the 295-K perturbation function shown in Fig. 2. The parameters obtained from the fit were used except that the line-shape parameter δ_1 was set equal to zero. The comparison of the two lines (for $\delta_1 \cong 0.1$ and $\delta_1 = 0$) illustrates the large amount of line broadening that is associated with the interactions at the Ti site in $PbTiO_3$.

Figure 4 presents several perturbation functions for a $CdTiO_3$ sintered pellet prepared in the ilmenite structure. With the exception of the function measured at 1260 K, which was fit using a two-site model, all of the functions were fit using a one-site model. The quality of the fits is very good. The derived values of A_1 and A_3 and chemical considerations indicate that 90±3 percent of the probes occupied the Ti site.

Figure 5 presents several perturbation functions for a $CdTiO_3$ sintered pellet prepared in the perovskite structure. These functions were measured on a single sample in which the temperature was increased successively from 295 to 1270 K. Although the 295- and 525-K data show a small indication of a second site, the two-site model was not necessary to obtain acceptable fits. But, for the data obtained at higher temperatures, the two-site model was necessary. To understand this effect, we prepared additional samples in both the perovskite and ilmenite structures. Some of the other $CdTiO_3$ perovskite samples showed an appreciable population of a second site at laboratory temperature. Whereas, the $CdTiO_3$ ilmenite samples showed essentially no population of a second site over the temperature range from 295 to 1050 K. Interestingly, at 77 K, the $CdTiO_3$ ilmenite sample showed a significant population of a second site, which we discuss in the following.

One explanation for the presence of a second site in the perovskite samples is that the effects of Cd volatility were not completely controlled. Loss of small amounts of either Cd or CdO from the structure produced a second chemical environment for the $^{181}Hf/^{181}Ta$ probe atoms. To verify this effect, firstly, we irradiated a pellet of perovskite $CdTiO_3$ to produce some ^{115}Cd activity; and secondly, we sealed this pellet in a long, evacuated fused-silica tube and heated it at a temperature of about 1400 K for a period of about one day. After this treatment, the

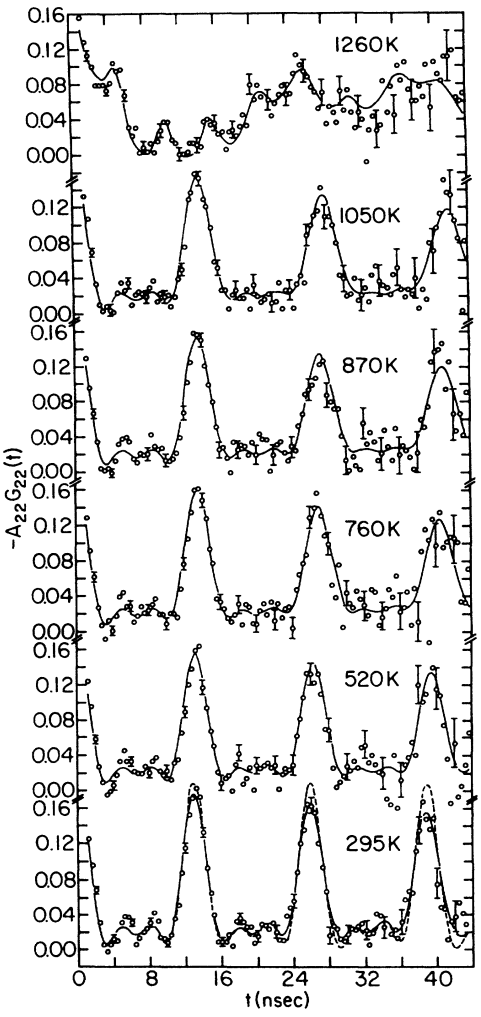

FIG. 4. Perturbation functions for $CdTiO_3$ prepared in the ilmenite structure and measured at the indicated temperatures. The solid lines represent least-squared fits to the data in which all but the function measured at 1260 K were fit with a one-site model. On the data measured at 295 K, the dotted line indicates a fit in which $\delta = 0$ and the other parameters are the same as for the solid line fit.

tube showed a large amount of ^{115}Cd radioactivity at the end of the tube that was not in the hot zone of the furnace. In this end of the tube, the deposition of brownish-black CdO was clearly visible. Similarly, the region of the tube that was in the hot zone showed very little ^{115}Cd radioactivity.

To illustrate the extent of this effect, Fig. 6(a) presents a typical perturbation function for a $CdTiO_3$ perovskite sample. The fits to the high-temperature data in Fig. 5 and to the data in Fig. 6(a) yielded consistent, unique frequencies for the primary site. But, for the much less populated secondary site, the fits yielded frequencies that corresponded to $\eta \cong 0$ and to $\eta \cong 1$. The quality of the fits was similar in either case, and no criteria were available to choose one set of frequencies over the other. Thus, despite the difficulties produced by the second site, the information derived from the data about the primary interactions was not sensitive to the details of the parameters derived for the second site. Also, the increase in the ingrowth of the second-site population with temperature that Fig. 5 shows simply resulted from Cd volatility that occurred during the experiment.

In the context of temperature effects, we call attention to the 1260-K perturbation function for the $CdTiO_3$ ilmenite sample and the 1270-K perturbation function for the $CdTiO_3$ perovskite sample, which Figs. 4 and 5 show, respectively. For both functions, the derived frequencies are alike, well within experimental error. This result indicates that over a temperature range from approximately 1050 to 1260 K the ilmenite phase underwent a transi-

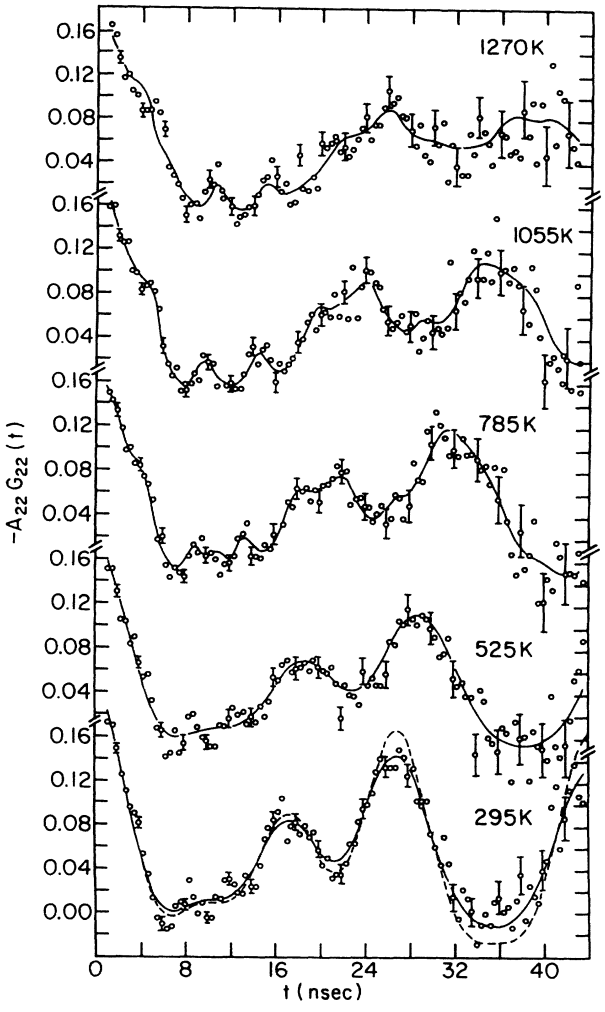

FIG. 5. Perturbation functions for $CdTiO_3$ prepared in the perovskite structure and measured at the indicated temperatures. The solid lines represent least-squared fits to the data. The two functions measured at 295 and 525 K were fitted using a one-site model in which the average site occupancy for the primary site was 91±2 percent. For the functions measured at the higher temperatures, a two-site model gave a better representation of the data. For the second site, acceptable fits were obtained for either $\eta=0$ or $\eta=1$ when $\omega_1=1400\pm30$, 1290 ± 30, and 1200 ± 40 Mrad/sec for the data obtained at 785, 1055, and 1270 K, respectively. For the $\eta \cong 1$ fits, the average primary site occupancy was 73±9 percent; and for the $\eta \cong 0$ fits, the average primary site occupancy was 80±10 percent. On the data measured at 295 K, the dotted line indicates a fit in which $\delta=0$ and the other parameters are the same as for the solid line fit.

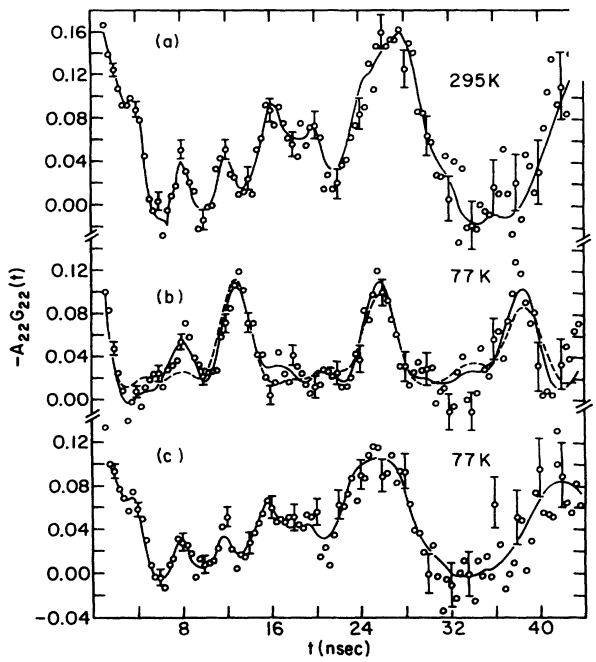

FIG. 6. (a) Perturbation function for a typical sample of $CdTiO_3$ prepared in the perovskite sample. The primary site occupancy was 73±7 percent. The fit converged at $\eta \cong 1$ for the second-site interaction in which $\omega_1=1538\pm22$ Mrad/sec. A fit that converged at $\eta \cong 0$ for the second-site interaction, in which ω_1, was approximately the same, yielded a primary site occupancy of 65±10 percent. Although the primary site frequency parameters are not affected significantly by convergence difficulties associated the secondary site, the normalization and line-shape parameters are affected. (b) Perturbation function for a sample of $CdTiO_3$ prepared in the ilmenite structure and measured at 77 K. The solid line is a two-site model fit, and the dotted line is a one-site model fit. (c) Perturbation function for a sample of $CdTiO_3$ prepared in the perovskite structure and measured at 77 K.

tion to the perovskite phase. Although the details of the transition were not clear, the transition most likely must have been reconstructive, because Cd was six coordinate in the ilmenite structure and twelve coordinate in the perovskite structure.

Figure 6(b) shows the 77-K perturbation function for a $CdTiO_3$ ilmenite sample. Unlike the 295-K functions, this one shows a second interaction which appears as a peak at 8 nsec and which is attenuated with time. This second interaction, which did not yield unique parameters, did not affect significantly the accuracy with which the primary site parameters were determined. For the purposes of comparison, Fig. 6(c) presents the 77-K perturbation function for the $CdTiO_3$ perovskite sample. Although this function does indicate two probe sites, it is qualitatively very similar to the 295 K function. In contrast, we did not expect the appearance of a second site at 77 K for the ilmenite phase. This result is interesting because in 1952 (Ref. 10) and later[11] the possibility of a transition to a ferroelectric phase at 50 K in $CdTiO_3$ was discussed. We would expect a transition of this type to occur from the perovskite phase, since perovskite structures are associated with ferroelectricity. But, the appearance of a second site in the 77 K data for ilmenite structure, which should not have been caused by Cd volatility, may be related to the onset of a phase transition. Currently, we are performing low-temperature measurements on samples of perovskite and ilmenite $CdTiO_3$.

For $CdTiO_3$ in the perovskite and ilmenite phases, Figs. 7(a) and 7(b) summarize the EFG parameters, V_{zz} and η, and the line-shape parameters, δ, respectively. For the perovskite phase, the line-shape parameters range from approximately 0.04 to 0.06 (excluding the 1270-K point) and they have large uncertainties. For the ilmenite phase, the line-shape parameters range from approximately 0 to 0.04. Thus, the line-shape parameters for neither phase approach the magnitudes of those obtained for the ferroelectric perovskite $PbTiO_3$, although the line-shape parameters for the ilmenite phase are systematically smaller than those for the perovskite phase. For the perovskite phase, the asymmetry parameters are close to 0.4, and they increase slowly with temperature. These asymmetries are consistent with and expected from the orthorhombic distortion of the perovskite structure.[12] For the ilmenite phase, the asymmetry parameters have relatively small values near zero, and these values are also consistent with and expected from the axial symmetry of the ilmenite structure.[13]

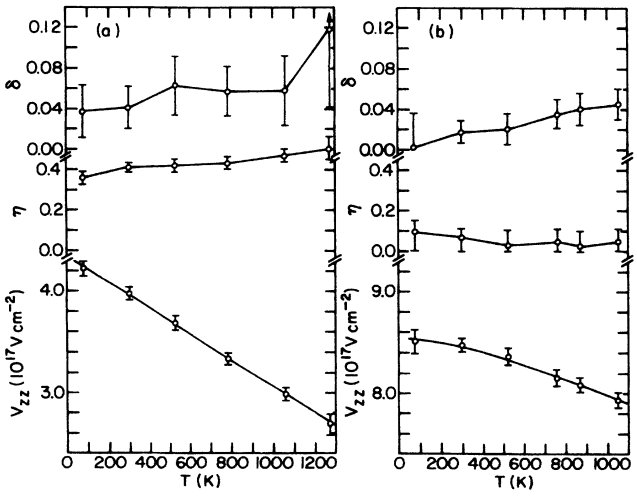

FIG. 7. Electric-field-gradient parameters and line-shape parameters for the primary interaction in $CdTiO_3$; (a) the perovskite phase and (b) the ilmenite phase. For the asymmetry parameters and line-shape parameters, the lines are drawn to guide the eye. For the EFG, the lines represent a least-squared fit to a straight line for the perovskite data and a fit to $V_{zz}(T)=a-bT^{3/2}$ for the ilmenite data.

IV. DISCUSSION

A. Temperature dependence of the EFG

Traditionally, the theoretical analysis of the EFG temperature dependence has focused on metals. Insulators and semiconductors have received little attention. We reviewed this situation in some detail in an earlier report.[9] For metals, the result of the analyses is that the EFG generally decreases with the three-halves power of the temperature: $V_{zz}(T)=a-bT^{3/2}$. For insulators, no functional dependence has been found either theoretically or empirically to have a widespread applicability. To analyze the temperature dependences of the Zr-site EFG's in the ionic-conducting ceramics, $CaZr_4P_6O_{24}$ and $SrZr_4P_6O_{24}$, we found that the Gaussian function: $V_{zz}(T)=\exp(-bT^2)$ provides a good representation of the data.[9,18]

Since $PbTiO_3$ is ferroelectric and highly polar in the tetragonal phase, we do not expect any conventional theory to apply *a priori*. Moreover, from measurements on ferroelectric $PbHfO_3$, Yeshurun, Havlin, and Schlesinger[8] observed that the EFG changed critically with temperature near T_c. Thus, we expect no single expression to provide a good representation of the Ti site EFG in $PbTiO_3$ over the entire temperature range that corresponds to the tetragonal phase. To fit the EFG temperature dependence shown in Fig. 3, we used the two indicated functions: The curves shown in Fig. 3 indicate that the fits are poor. For the purposes of comparison, we selected a set of EFG values that corresponded to temperatures well below T_c $T<600$ K, and both functions represent the data reasonably well. Thus, when $T \ll T_c$, the apparent good agreement of both expressions with the EFG temperature dependence indicates that the functions represent little physical information.

Unlike the $PbTiO_3$ case, the case of $CdTiO_3$ is not complicated by ferroelectric effects. More importantly, the $CdTiO_3$ case provides an opportunity to examine the same compound in two different phases over the same temperature range. For the perovskite phase, the fit shown in Fig. 7(a) indicates that the EFG temperature dependence is strictly linear. For the ilmenite phase, the data shown in Fig. 6(b) indicate that the EFG temperature dependence is nonlinear, and the fit of the power-law expression to the data indicates that it is a reasonably good representation. Unfortunately, the fit of the Gauss-

ian expression, which is not shown, also provides a representation that is just as good. To obtain physical information directly from the EFG temperature dependence will require more sophisticated models.

B. Line-broadening phenomena

Traditionally, the theory of Abragam and Pound[19] has been used to describe nuclear-spin relaxation produced by rapidly fluctuating EFG's. This particular model describes the fluctuations of an axially symmetric EFG in terms of a correlation time τ_c and an average root-mean-square quadrupole frequency $\langle\omega_Q^2\rangle^{1/2}$, in which $G_{22}(t)=\exp(-\lambda_{22}t)$ and $\lambda_{22}=100.8\langle\omega_Q^2\rangle\tau_c$ for spin $I=\frac{5}{2}$. This expression for the perturbation function is rigorously valid when $\langle\omega_Q^2\rangle^{1/2}\tau_c \ll 1$. In the absence of any static interactions, this model gives a simple attenuated perturbation function. When static interactions are also present, the general approach is to multiply expressions that are similar to the right-hand side of Eq. (1) by $\exp(-\lambda_{22}t)$.

Because the time scales of motion of various species can vary over many orders of magnitude in solid-state systems, this approach is inherently limited. In particular, to be valid, firstly, $\langle\omega_Q^2\rangle^{1/2}\tau_c \ll 1$; and, secondly, the line-broadening factors in Eq. (1), $\exp(-\frac{1}{2}\delta\omega_k t_i)$, need to represent accurately only the effects of static inhomogeneities such as impurities and point defects. Gardner *et al.*[20] used both the ^{181}Hf/^{181}Ta and the ^{111}In/^{111}Cd PAC probes to study zirconia solid solutions at high temperatures. Indeed, they analyzed measurements on high-temperature (tetragonal) zirconia, and they found that using a Gaussian line-broadening factor $\exp[-\frac{1}{2}(\delta\omega_k t)^2]$ and using no premultiplication by an attenuation factor ($\lambda_{22}=0$) produced an accurate representation of some of their data. Whereas, using only the attenuation factor and using no linebroadening factor ($\delta=0$) to analyze the same data produced a significantly poorer representation of the data. For these zirconia data, the derived δ parameters showed a strong temperature dependence. For this reason and others, Gardner *et al.*[20] interpreted the line broadening as having resulted from a fluctuating EFG. This particular experiment[20] showed that, under appropriate conditions, interactions of the probes with fluctuating EFG's can produce line broadening, which is not accompanied by any significant amount of attenuation. Moreover, in solids, depending on the rate of fluctuation, interactions with fluctuating EFG's can produce either attenuation or broadening effects. The stochastic model developed by Winkler and Gerdau[21] (which is based in part on Blume's model[22]) supports this conclusion (see Fig. 1 in Ref. 21). Now, we expect interactions with fluctuating EFG's in either $PbTiO_3$ or $CdTiO_3$ measured at relatively low temperatures to have very different origins from those interactions with fluctuating EFG's measured at high temperatures in tetragonal zirconia. Nonetheless, this discussion sets the context in which to analyze the $PbTiO_3$ and $CdTiO_3$ perturbation function.

The major issue that concerns interpreting the line broadening in these perturbation functions is whether the effect arose either from nuclear-spin relaxation caused by a fluctuating EFG or from static inhomogeneities, or from both. For ferroelectric $PbTiO_3$, at temperatures below T_c, the line broadening is reasonably large at low temperatures, $\delta\cong 0.1$, and it increases rapidly near T_c. For nonferroelectric $CdTiO_3$ in both phases, the line broadening is relatively small, $\delta<0.04$, and it shows no clear temperature sensitivity. In addition, the perturbation functions for both compounds indicate that a small fraction of the probes were in poorly defined chemical locations, i.e., $A_3>0$. Generally, the fitting procedure does not completely separate the effects of changes in δ_1, δ_2, A_1, A_2, and A_3. As a result, the line-shape parameters derived from the measured perturbation functions for $CdTiO_3$ and to a lesser extent for $PbTiO_3$ are uncertain and not completely unique. This problem is further exacerbated by the fact that the line-broadening factors $\exp(-\frac{1}{2}\omega\delta_k t_i)$ in Eq. (1) are purely phenomenological and do not imply a specific physical mechanism for the line broadening.

To address this situation, we consider the line broadening associated with the two $CdTiO_3$ phases. The perovskite and the ilmenite phases were prepared from either the same powder or powders made from the same process. Thus, the impurity content would have been common to both phases. Similarly, defects such as oxygen vacancies, that would have resulted from the charge compensation of acceptor impurities such as either Al^{3+} or Fe^{3+}, also would have been common to both phases. At low temperatures, oxygen vacancies would have been immobile; and cation transport would not have occurred. Over the temperature range of interest below 1200 K, the line-shape parameters corresponding to either $CdTiO_3$ phase show little change with increasing temperature. Although the line-shape parameters for the two phases differ somewhat in magnitude, the parameters are small and the differences could be an artifact of the data fitting process. These line-shape features of the $CdTiO_3$ phases are consistent with static inhomogeneous line broadening.

If the defect content and the defect chemistry were the same in the perovskite $CdTiO_3$ sample and in the perovskite $PbTiO_3$ samples, then it would be plausible to attribute most of the line-broadening effects shown by $PbTiO_3$ to the effects of nuclear-spin relaxation. There are some similarities in the two species. Both compounds crystallized in distorted ABO_3 perovskite structures. The major difference in composition is the identity of the A ion, since the $CdTiO_3$ and $PbTiO_3$ samples were prepared in the same laboratory in which the same process was used. The impurity content of both types of samples was very likely to be similar. But, unfortunately, chemical differences between the Cd^{2+} and Pb^{2+} ions and structural differences in the respective unit cells could have produced quite different distributions of static inhomogeneities. Alternatively, the defect structures could have been similar. So, the line broadening shown in the $PbTiO_3$ perturbation functions for low temperatures cannot be attributed to a singular static mechanism.

Despite the limitations in the data, we consider the

case of static inhomogeneous line broadening further. The effect arises because static defects are distributed throughout the crystal, and the effect is characterized by a distribution of interaction frequencies. A simple model of the process is to consider the measured EFG as being comprised of two components: (1) a component that represents the interaction of the probe nucleus with the other normal constituents of the lattice and (2) a component that represents the interactions of the probe nucleus with the defects. The former component is temperature dependent and affects the mean of the frequency distribution; whereas, the latter component is temperature insensitive and produces the width in the frequency distribution. To determine whether this model describes the observed line broadening, we examine the absolute width, $\Delta\omega$, of the frequency distribution from which the line-shape factors were derived. Figure 8 presents the absolute widths, $\Delta\omega=\omega_1\delta$, which were obtained from the parameters, ω_1 and δ, that were derived from the fits to the $PbTiO_3$ perturbation functions. The widths were obtained using both the Lorentzian and the Gaussian line-shape factors. Both factors show the same qualitative temperature dependence. For temperatures below 600 K, the widths are essentially temperature insensitive. But, at higher temperatures, the widths increase with as the temperature approaches T_c. Thus, at temperatures near T_c, the relative width δ increases more rapidly than ω_1 decreases. In this temperature range, the rapid decrease of the EFG is consistent with the onset of critical behavior. The rapid increase of the line-shape parameter in this temperature range strongly suggests that dynamic nuclear-spin relaxation may have occurred. At temperatures near T_c, this argument supports a spin-relaxation mechanism for tetragonal ferroelectric $PbTiO_3$ in which the Ti ion jumped between locations that corresponded to minima on a potential-energy surface. At lower temperatures, the measured line broadening provides insufficient information to distinguish the contributions that resulted from dynamic spin relaxation and those that resulted from static inhomogeneities.

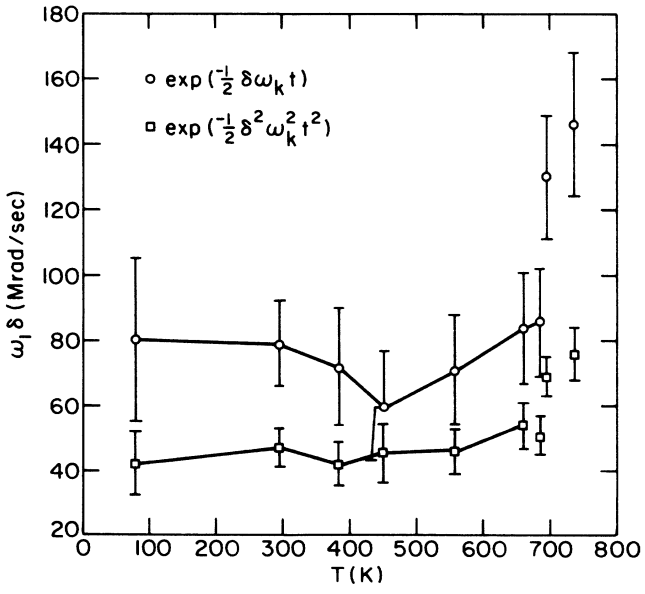

FIG. 8. Temperature dependence of the absolute width; $\Delta\omega=\omega_1\delta$, for $PbTiO_3$. The line-shape factors for a Lorentzian distribution and for a Gaussian distribution were used in Eq. (1) to obtain the widths. The lines are drawn to guide the eye.

In the context of this possible spin-relaxation mechanism, we recognize that a distinction must be made between the hopping of Ti ions and the hopping of ^{181}Ta probe ions, since clearly the two species have different masses and valences. However, similar linebroadening phenomena have been observed in ABO_3 perovskites that have heavier B ions such as $PbHfO_3$.[23] Thus, some experiments should be performed to delineate the differences in the measured interactions that arise from nonindigenous probes such as ^{181}Ta in $PbTiO_3$. For example, a study that compares interactions in $KNbO_3$ to those in $KTaO_3$ using the $^{181}Hf/^{181}Ta$ probe may address this question.

V. CONCLUSIONS

The PAC measurements on the tetragonal, ferroelectric phase of $PbTiO_3$ showed marked line broadening that increased significantly at temperatures near T_c. On ilmenite and perovskite $CdTiO_3$, the measurements, which were made over a greater temperature range, showed significantly less line broadening. A simple picture of the effects of static inhomogeneities on the line shapes suggests that the absolute frequency width, $\Delta\omega$, should remain relatively constant over the range of temperatures. Because the absolute widths associated with the $PbTiO_3$ perturbation functions increased at temperatures near T_c, the corresponding broadening of the lines may have resulted from a dynamic spin-relaxation mechanism. The extent of dynamic spin relaxation at lower temperatures is not clear.

The question remains as to the cause of the fluctuating EFG in $PbTiO_3$. In the order-disorder model, the Ti ions are located at potential-energy-surface minima that are off of the crystallographic Ti site. Therefore, at low temperatures, relatively infrequent hopping of probe ions from minimum location to minimum location could have produced the EFG fluctuations that contributed to the line broadening. At temperatures that approached T_c, the hopping rates could have increased rapidly but not rapidly enough to have produced motional narrowing. This increase in fluctuation rate could have been responsible for the observed increase in line broadening.

Conventional expressions could not describe uniquely the temperature dependence of the EFG at the Ti site in ferroelectric, tetragonal $PbTiO_3$. This result is neither unusual nor unexpected, because the lattice vibrations are very anharmonic in ferroelectric perovskites. Perhaps, more importantly, the rapid change of the EFG with temperature near T_c indicated the onset critical behavior. but, better sample temperature control is needed to measure accurately the critical changes in the EFG as the temperature approaches T_c. The EFG at the Ti site in perovskite $CdTiO_3$ decreased linearly with temperature,

and this effect is anomalous. Whereas, the EFG at the Ti site in ilmenite $CdTiO_3$ decreased slowly with temperature in a not unusual way.

ACKNOWLEDGMENTS

We thank Professor Robert L. Rasera of the University of Maryland Baltimore County for critically reading the manuscript and for offering several very helpful suggestions. For various suggestions, comments, and discussions, we would like to thank Professor John A. Gardner of Oregon State University, Professor William E. Evenson of Brigham Young University, and Professor Morton Kaplan of Carnegie-Mellon University. We thank Professor Stewart K. Kurtz, Director of the Materials Research Laboratory, for suggesting that we use PAC spectroscopy to study order-disorder phenomena in ferroelectric materials. We also thank Professor Kurtz for providing technical assistance and much encouragement. We greatly appreciate the assistance that Professor William B. White provided by explaining some of the nuances of crystal chemistry and symmetry to us.

[1]M. E. Lines and A. M. Glass, *Principles and Applications of Ferroelectrics and Related Materials* (Oxford University Press, Oxford, 1977).

[2]W. Cochran, Adv. Phys. **9**, 387 (1960).

[3]See, for example, G. Burns and B. A. Scott, Phys. Rev. B **7**, 3088 (1973).

[4]J. P. Sokoloff, L. L. Chase, and D. Rytz, Phys. Rev. B **38**, 597 (1988).

[5]R. Comes, M. Lambert, and A. Guinier, C. R. Acad. Sci. (Paris) **226**, 959 (1968).

[6]R. Comes, M. Lambert, and A. Guinier, Solid State Commun. **6**, 715 (1968).

[7]G. L. Catchen, S. J. Wukitch, E. M. Saylor, W. Huebner, and M. Blaszkiewicz, Ferroelectrics (to be published).

[8]Y. Yeshurun, S. Havlin, and Y. Schlesinger, Solid State Commun. **27**, 181 (1978).

[9]See, for example, the discussion of the EFG temperature dependence in insulators, G. L. Catchen, L. H. Menke, M. Blaszkiewicz, K. Jamil, D. K. Agrawal, W. Huebner, and H. A. McKinstry, Phys. Rev. B **37**, 4839 (1988).

[10]G. A. Smolenskii, Dok. Akad. Nauk SSSR **85**, 985 (1952).

[11]F. Jona and G. Shirane, *Ferroelectric Crystals* (MacMillan, New York, 1962), pp. 152–253.

[12]H. F. Kay and J. L. Miles, Acta Crystallogr. **10**, 213 (1957).

[13]T. F. W. Barth and E. Posajak, Z. Kristallogr. **88**, 265 (1934); *X-ray Powder Diffraction Files,* 1989, edited by W. F. McClure (JCPDS International Centre for Diffraction Data, Philadelphia, 1989), Vol. 29, Entry 277.

[14]See, for example, P. A. Lessing, Ceramic Bull. **68**, 1002 (1989).

[15]G. L. Catchen, L. H. Menke, Jr., K. Jamil, M. Blaszkiewicz, and B. E. Scheetz, Phys. Rev. B **39**, 3826 (1989).

[16]G. L. Catchen, Hyperfine Interactions **52**, 65 (1989).

[17]G. L. Catchen, Comput. Phys. Commun. **55**, 85 (1989).

[18]G. L. Catchen, M. Blaszkiewicz, L. H. Menke, K. Jamil, H. A. McKinstry, D. K. Agrawal, and W. Huebner, Phys. Rev. B **37**, 7189 (1989).

[19]A. Abragam and R. V. Pound, Phys. Rev. **92**, 943 (1953).

[20]J. A. Gardner, H. Jaeger, H. T. Su, W. H. Warnes, and J. C. Haygarth, Physica B **150**, 223 (1988), and references therein.

[21]H. Winkler and E. Gerdau, Z. Phys. **262**, 363 (1973).

[22]M. Blume, Nucl. Phys. **A167**, 81 (1971).

[23]M. Forker, A. Hammesfahr, A. Lopez-Garcia, and B. Wolbeck, Phys. Rev. B **71**, 1039 (1973).